Schweizerische Eidgenossenschaft
Confédération suisse
Confederazione Svizzera
Swiss Confederation

12th European Conference on Severe Storms – ECSS2025
Utrecht, Netherlands
17 – 21 November 2025

Federal Department of Home Affairs FDHA
Federal Office of Meteorology and Climatology MeteoSwiss

The Devastating Convective Wind Event of 24 July 2023 in La Chaux-de-Fonds, Switzerland : Causes, Probable Mesoscale and Storm-Scale Mechanisms at Play and Nowcasting Implications

Lionel Peyraud [1], Aude Untersee [1], Stephan Vogt [2], Marco Stoll [1], Barbara Galliker [3], Isabelle Bey [1] Pamela Probst [4]
Federal Office of Meteorology and Climatology, MeteoSwiss, [1] Forecasting & Consulting / [2] Measurements & Data Integration / [3] Communications / [4] W4UN, Geneva / Zürich, Switzerland

1. Introduction

- ❑ On 24 July 2023, a **low-topped (LT) high-precipitation (HP) supercell thunderstorm** struck the city of **La Chaux-de-Fonds** in the Jura mountains of northwest Switzerland
- ❑ **Impact** : **1 fatality, 45 injuries, > 135 million Swiss Francs** of material damages, **~ 22,000 trees** torn down, **~ 3,000 buildings** damaged, **deep psychological trauma** inflicted on inhabitants
- ❑ Validated **1-sec max convective wind gust of 60,4 m/s (217 km/h)** measured at the SwissMetNet ground station at Eplatures regional airport with **widespread IF2 damages** within a 6 km x 2 km ellipse
- ❑ **Extensive post-event analysis** conducted to determine the storm-scale origin of the violent convective wind gusts given the weaker than average reflectivity intensity on radar.
- ❑ Multiple data platform analysis points to a **hybrid wind event** composed of both a **microburst and a tornado** due to specific spatial/temporal **phasing of convective processes at the storm scale**.

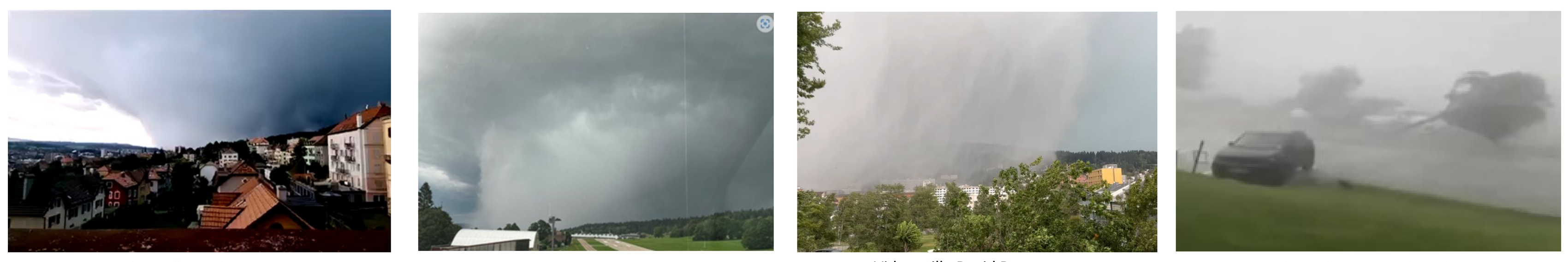

Fig. 1 : Photos and video stills of the low-topped high-precipitation supercell thunderstorm approaching La Chaux-de-Fonds on the morning of 24.07.2023

Fig. 2 : Photos of the structural and vegetation damages in and around the city of La Chaux-de-Fonds inflicted by the convective wind gusts following the passage of the storm.

2. Methodology

- ❑ A **thorough post-event analysis** was conducted composed of a **platform of multi-sourced data** and utilizing a **top-down method**, funneling down from the **synoptic to the mesoscale to the storm-scale**.

Post-event analysis composed of multiple data sources

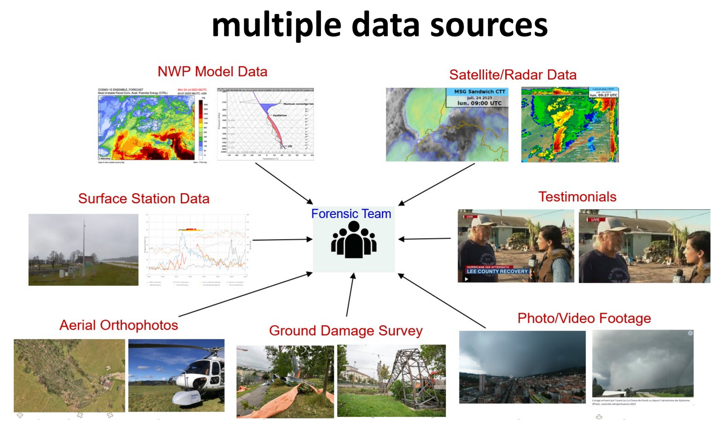

Fig. 3 : Various data sources utilized in the post-event analysis to identify the underlying atmospheric processes at play in this extreme convective wind event (Source : MeteoSwiss)

Convective post-event analysis conducted top-down from the synoptic scale down to the storm-scale

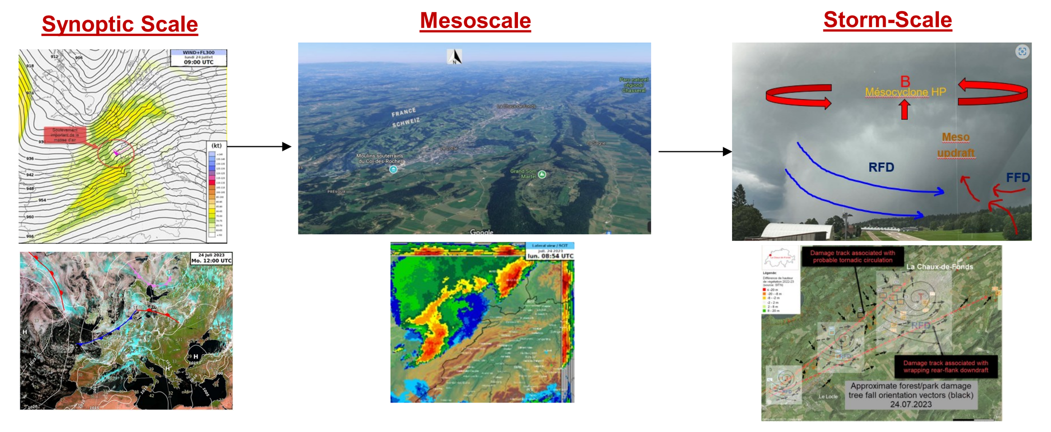

Fig. 4 : Left: Large-scale drivers of the convective event with upper-level double jet configuration (left exit+right entrance) and approaching low-level CFROPA. Middle : Mesoscale convective evolution and interaction with the Jura topography. Right : Phasing of specific meteorological parameters at the storm-scale (Source : MeteoSwiss)

- ❑ **Cooperation between MeteoSwiss, local authorities and specialized agencies** was crucial in obtaining a realistic and comprehensive picture of what transpired and was determinant in **identifying the meteorological phenomena involved**

Schweizerische Eidgenossenschaft / Confédération suisse / Confederazione Svizzera / Confederaziun svizra — Office fédéral de météorologie et de climatologie MétéoSuisse
ne.ch
RÉPUBLIQUE FRANÇAISE — METEO FRANCE
European Severe Storms Laboratory
SITN GÉOPORTAIL DU SYSTÈME D'INFORMATION DU TERRITOIRE NEUCHÂTELOIS

3. Results

Meteorological Context & Ingredients

Instability & Vertical Wind Shear — **Large-scale Lift**

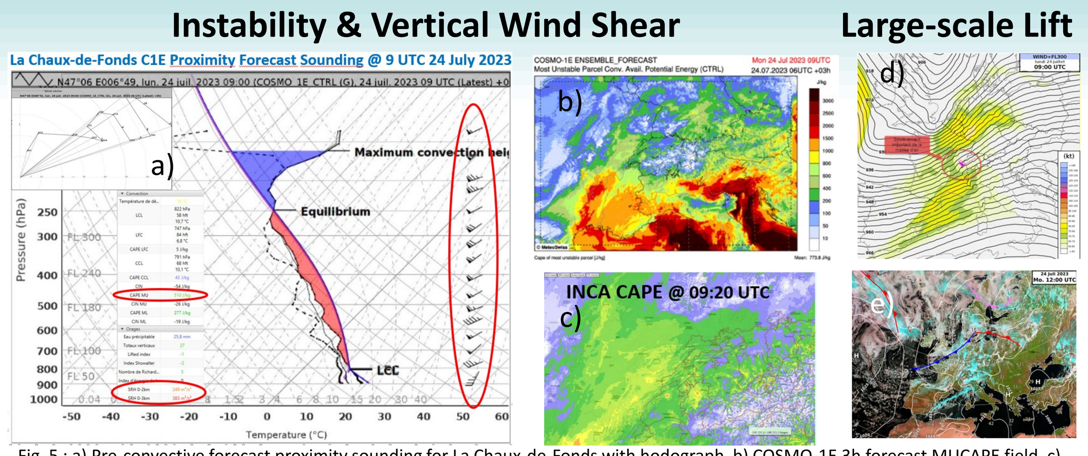

Fig. 5 : a) Pre-convective forecast proximity sounding for La Chaux-de-Fonds with hodograph. b) COSMO-1E 3h forecast MUCAPE field. c) Real-time INCA CAPE. d,e) Upper-level coupled jet configuration and low-level airmasses (Source : COSMO-1E NWP, MeteoSwiss-APN)

- ❑ Instability : **MUCAPE -> 400-1200 J/kg** (low CAPE)
- ❑ Vert. wind shear : **0-6km : 50-65 kts ; 0-3 km : 40-60 kts** (High Shear)
- ❑ Large-scale lift : **double jet structure aloft + LL prefrontal warm sector**
- ❑ Low-level hodograph curvature : **0-2/3 km SRH -> ~ 250 - 390 m^2/s^2**

Upstream bow-echo phase — **LT HP supercell phase**

- ❑ **La Plaine Morte Doppler Radar data** (with hypothesized mechanisms)

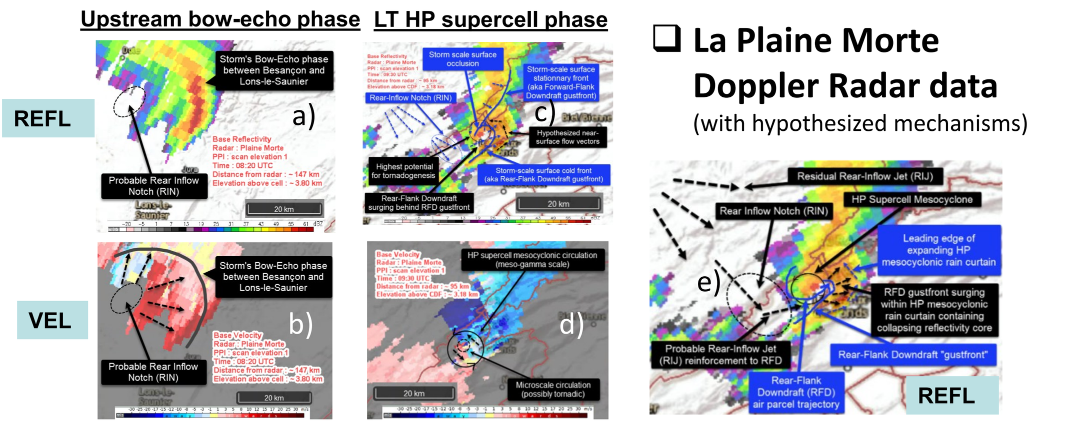

Fig. 9 : a,b) Storm's upstream bow echo phase in Vallée de la Saône. c,d,e) Storm's supercellular phase over La Chaux-de-Fonds as RFD was in the process of gusting out during Descending Reflectivity Core (DRC) collapse. Hypothesized storm-scale processes/mechanisms annotated in blue and black (Source : La Plaine Morte C-band radar, MeteoSwiss ; annotations : Lionel Peyraud)

SwissMetNet Extreme Wind Measurements

- ❑ La CDF : Les Eplatures airport
- ❑ **1-s wind gust : 60,4 m/s** (217 km/h)


Fig. 12 : SwissMetNet ground station at Les Eplatures airport in La Chaux-de-Fonds that recorded the extreme wind gusts (1-sec gust : 217 km/h) (Source : MeteoSwiss)

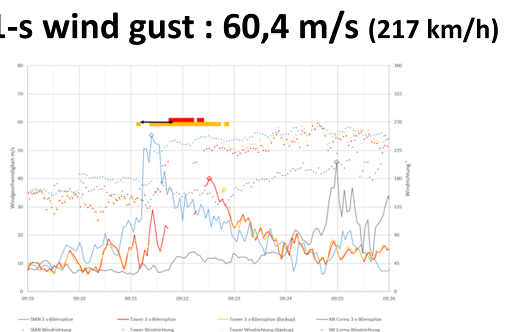
Fig. 13 : Various MeteoSwiss 3-sec anemometer readings (lines: speed, dots: direction) at Les Eplatures airport and Mont Cornu around La Chaux-de-Fonds. Max 3-sec reading was 57 m/s (198 km/h) at the airport (Source: MeteoSwiss)

Storm Characterization via Satellite / Radar

- ❑ **Montancy Radar Dopper velocity during LT HP supercell phase over La CDF** (triple PRF)

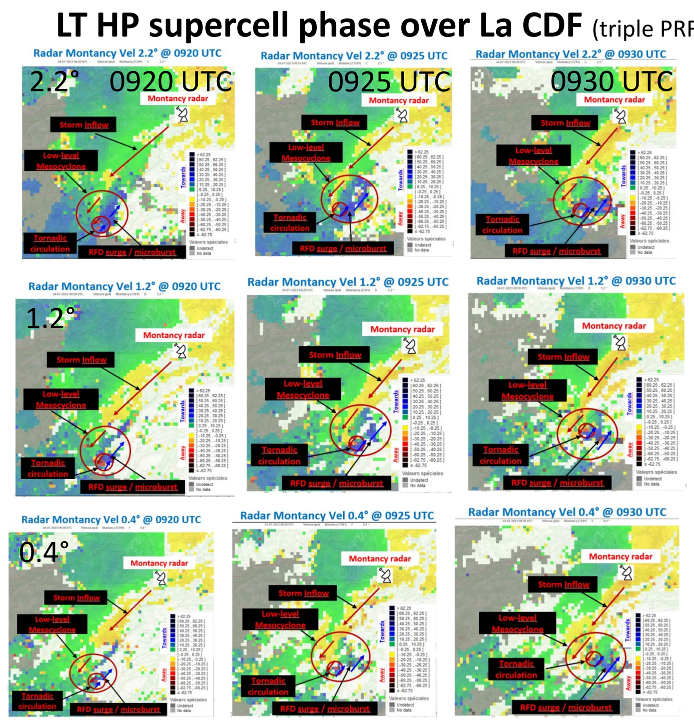

Fig. 6 : Montancy (FR) Doppler radar velocity scans at 2.2° (top), 1.2° (middle) and 0.4° (bottom) elevation angles between 0920-0930 UTC on 24.07.2023 with storm signatures annotated (Source : Montancy C-band radar, MétéoFrance / Michael Kreitz)

- ❑ **MSG sandwich product : Cold-U signature** during upstream **bow-echo phase**

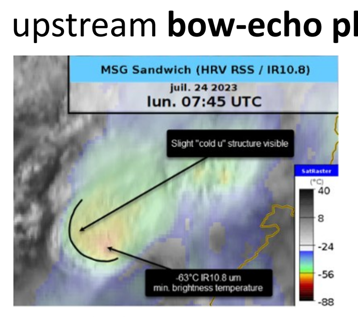

Fig. 7 : MSG sandwich (Source : EUMETSAT, MeteoSwiss)

- ❑ **Weak signatures** during **LT HP supercell phase**

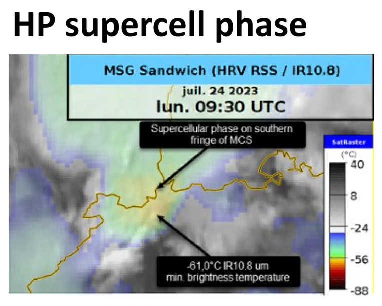

Fig. 8 : MSG sandwich (Source : EUMETSAT, MeteoSwiss)

- ❑ Radar detected storm signatures : **storm inflow, low-level mesocyclone, hook echo, microscale circ. (possible TVS), RFD surge (microburst), bowing phase**

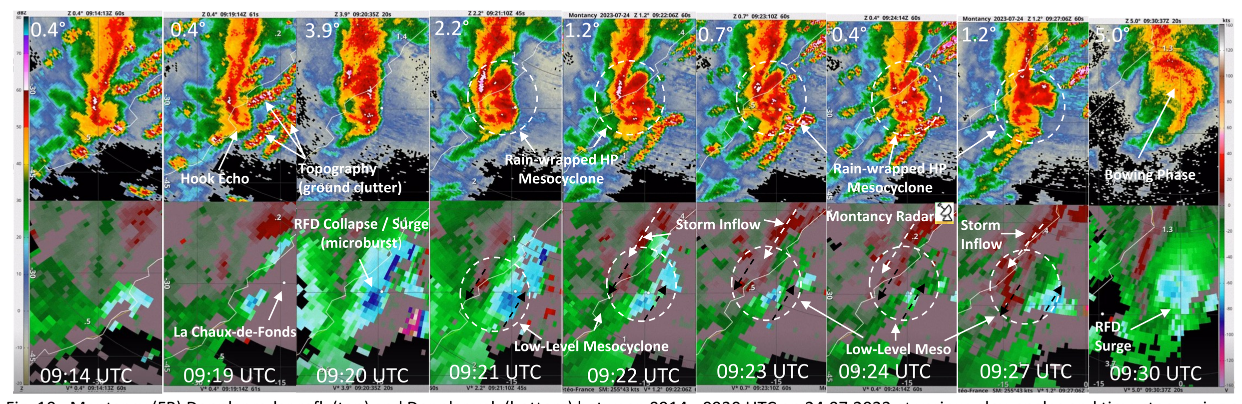

Fig. 10 : Montancy (FR) Doppler radar refl. (top) and Doppler vel. (bottom) between 0914 - 0930 UTC on 24.07.2023 at various elev. angles and time steps using a triple-PRF scan strategy as the low-topped HP supercell was impacting La Chaux-de-Fonds (Source : MétéoFrance & Bram van't Veen radar data displayer, ESSL)

- ❑ **Descending Reflectivity Core (DRC)** visible in vertical cross-sections / RHI

Fig. 11 : MeteoSwiss radar network CAPPI vertical cross-section reflectivity scans between 0920-0935 UTC as low-topped HP supercell was impacting La Chaux-de-Fonds. Downward pointing arrow shows progressive reflectivity core collapse (Source : MeteoSwiss)

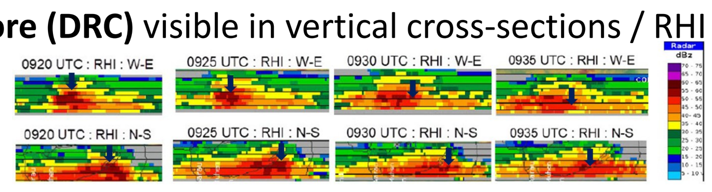

Storm Characterization via Visual Obs (photos/videos/testimonials)

- ❑ **Webcams/photos/videos** of approaching HP low-level mesocyclone circulation

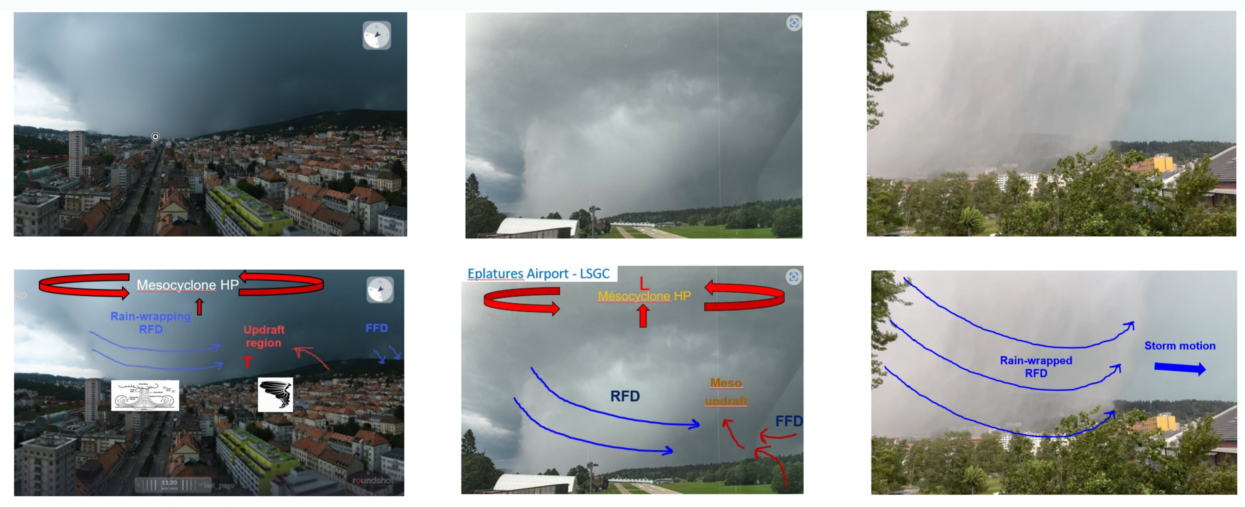

Fig. 14 : Webcam/photo/video stills of HP supercell rain-wrapped RFD circulation approaching the city of La Chaux-de-Fonds from the west on 24.07.2023. Animated video footage (not shown) clearly shows a broad cyclonic rotational aspect to the RFD rain curtains wrapping around the low-level mesocyclone. (Source : Roundshot.com webcam (left), Eplatures airport tower video still (center), David Deruns video still (right))

Damage Analysis (aerial/ground damage surveys, photos/videos)

- ❑ Southern side of town -> **unidirectional/divergent wind damage** (microburst)
- ❑ Northern side of town -> **multidirectional/convergent wind damage** (tornadic)

Fig. 15 : Unidirectional/divergent treefall wind damage in «Parc Gallet» on the southern side of the city, suggesting a downdraft-driven wind phenomenon (Source : SITN, NE-CH)

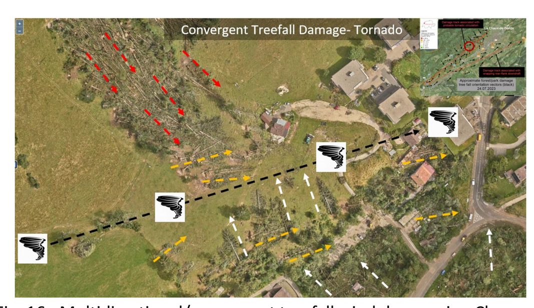

Fig. 16 : Multidirectional/convergent treefall wind damage in «Chapeau-Rablé» section along the northern fringe of the city, suggesting a updraft-driven convergent wind phenomenon (Source : SITN, NE-CH)

- ❑ **Int'l Fujita Scale -> IF-2 damage observed**

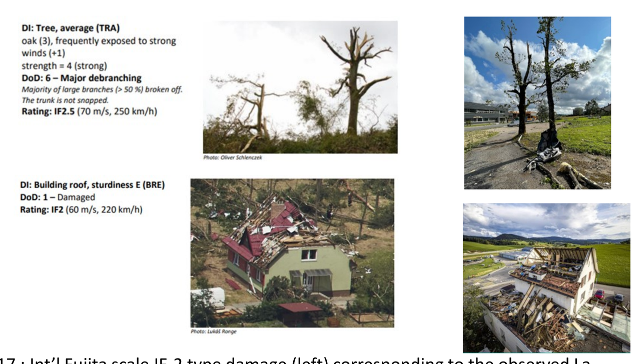

Fig. 17 : Int'l Fujita scale IF-2 type damage (left) corresponding to the observed La Chaux-de-Fonds wind damage on 24.07.2023 (right) (Source : ESSL Int'l Fujita Scale for tornado and wind damage assessments document)

- ❑ **Damage tracks** confirmed by **aerial/ground surveys**

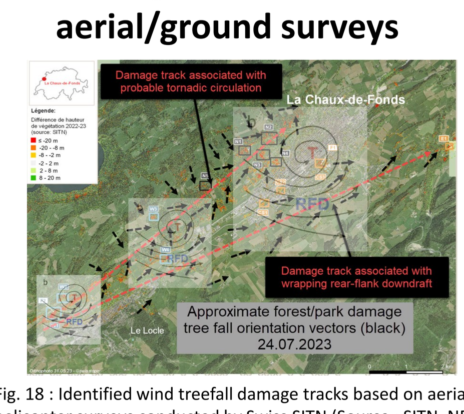

Fig. 18 : Identified wind treefall damage tracks based on aerial helicopter surveys conducted by Swiss SITN (Source : SITN, NE-CH)

4. Summary / Conclusions

Hypothesized Mesoscale & Storm-Scale Mechanisms at Play

CDF Event : Storm-Scale Processes Strongly Involved -> Nowcasting Challenge

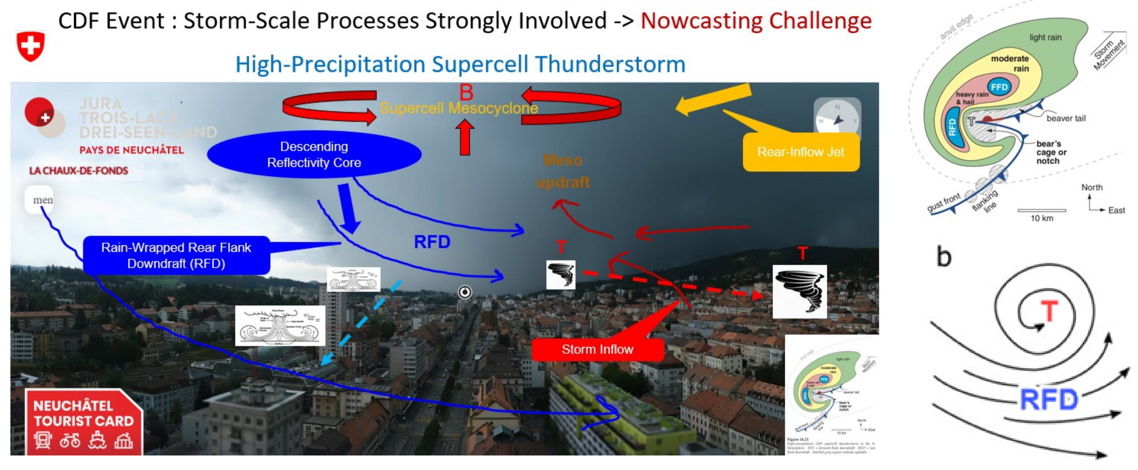

Fig. 19 : Left : Hypothesized mesoscale and storm-scale mechanisms at play, responsible for the extreme convective hybrid wind event in La Chaux-de-Fonds on 24.07.2023, composed of both an RFD generated wet microburst and a rain-wrapped tornadic circulation (Source : Roundshot.com, MeteoSwiss Lionel Peyraud). Upper right : conceptual model of a high-precipitation supercell (Source : Stull 2017). Lower right : Near-surface wind pattern b for a hybrid wind event adapted from «The International Fujita (IF) Scale for tornado and wind assessments» (Source : ESSL)

- ❑ Phasing at storm-scale : **Rear-Inflow Jet** (RIN)-> **Descending Reflectivity Core** (DRC)-> **Rear-Flank Downdraft** (RFD)-> Induced **microburst->** induced **tornadogenesis**
- ❑ **Topographical funneling** of mesoscale/storm-scale winds **in Jura valley**
- ❑ **City architecture wind funneling** due to **city grid style**
- ❑ **Low-level mesocyclone** was essentially **grazing the ground at 1000 m elevation**

NWP Performance, Warning Issuance & Nowcasting Implications

- ❑ **Severe thunderstorm outlook/watch** issued
- ❑ **COSMO-1E NWP-EPS fields very dispersed** and didn't capture true intensity
- ❑ **Radar-based algorithms didn't trigger a severe t-storm warning** as low-topped supercell had **below threshold reflectivity-based values**
- ❑ **Storm's mesocyclone detected by MeteoSwiss radar-based MDA in test phase**

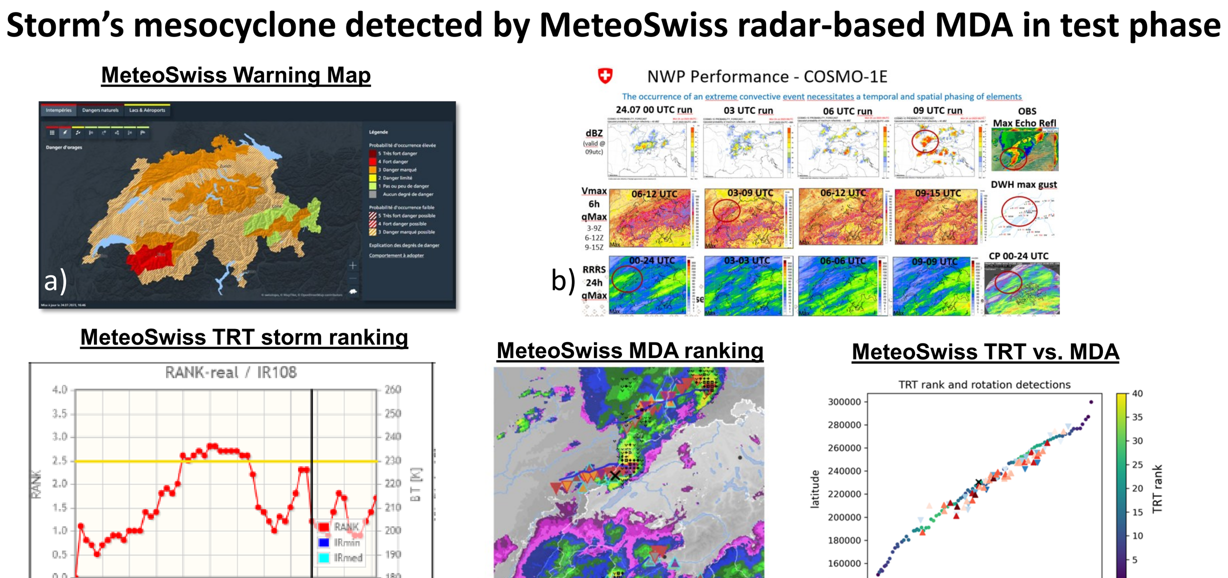

Fig. 20 : a) MeteoSwiss weather hazard warning map with an orange-stippled Severe Thunderstorm Outlook/Watch active over much of country on 24.07.2023. b) MeteoSwiss short-term NWP forecasting data for simulated dBZ, 6h max gusts and 24h QPF (Source : MeteoSwiss-MD-MDR). c) MeteoSwiss Thunderstorm Radar Tracking (TRT) algorithm ranking for storm's intensity (Source : MeteoSwiss-MD-MDR). d) Mesocyclone Detection Algorithm (MdATing) identifying a strong/intense mesocyclone with La Chaux-de-Fonds storm (Source : MeteoSwiss-MD-MDR, Monika Feldmann. e) TRT rank vs. MDA detection (Source : MeteoSwiss- MD-MDR, Monika Feldmann)

Jura Mountains : A Local Tornado Alley

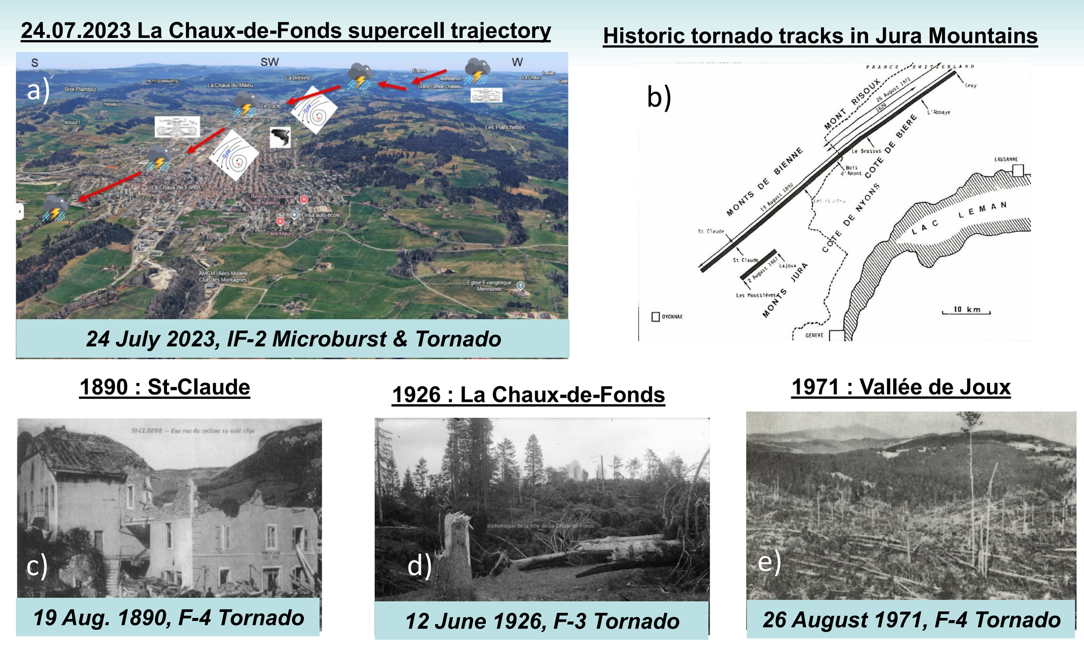

Fig. 21 : a) The low-topped HP supercell's trajectory as it relates to the Jura topography and the city grid (Source : Googlemaps). b) Historic tornadic storms over the Jura mountains in the past (Source : Dessens and Snow, 1993). c) Structural damage from the 19.08.1890 F-4 tornado in St. Claude (Photo : Vincent Vuillermoz) d) Forest damage from the 12.06.1926 La Chaux-de-Fonds F2-F3 tornado (Source : La Chaux-de-Fonds library) e) Forest damage in Vallée de Joux from the 26.08.1971 F-4 tornado (Photo : Daniel Aubert)

- ❑ **Several strong/violent tornadoes observed over the Jura since 17th century** -> 1624, 1768, 1842, 1890 (F-4), 1926 (F-2), 1967 (F-3), 1971(F-4)
- ❑ **Funneling of winds within SW oriented valleys** is hypothesized to **increase speed/directional low-level shear**
- ❑ **Convective cloud bases closer to ground** over the Jura seems determinant in **increasing tornadogenesis probability**

MeteoSwiss

References :

- Bluestein, H. B. and S. G. Gaddy, 2001: Airborne pseudo-dual-Doppler analysis of a rear-inflow jet and deep convergence zone within a supercell. Mon. Wea. Rev., 129, 2270–2289.
- Byko, Z., P. Markowski, Y. Richardson, J. Wurman and E. Adlerman, 2009 : Descending reflectivity cores in supercell thunderstorms observed by mobile radars and in a high-resolution numerical simulation. Wea. Forecasting, 24, 155-186.
- Dessens J, Snow JT. 1993. Comparative description of tornadoes in France and United States. The tornado: its structure, dynamics, prediction and hazards. Amer. Geofis. Union 427-434.
- Fujita, T. T., and R. M. Wakimoto, 1981 : Five scales of airflow associated with a series of downbursts on 16 July 1980. Mon. Wea. Rev., 109, 1438-1456.
- Gauthier, L., La trombe-cyclone du 19 août 1890, C. R. Hebd. Seances Acad. Sci., 111, 417-421, 1890.
- Groenemeijer, P., L. Bock, J. Soriano, M. Dutkiewicz, D. Gutiérrez-Rubio, A. M. Holzer, M. Hubrig, R. Kaltenberger, T. Kühne, M. Müller, B. Van Der Ploeg, T. Púčik, T. Schreiner, M. Singer, G. Strommer, A. Xhelaj, 2023 : The International Fujita (IF) Scale for tornado and wind damage assessments, version 1.0b. https: www.essl.org : European Severe Storms Laboratory e.V. [Online]
- Moller, A.R., Doswell III, C.A., Foster, M.P., Woodall, G.R., 1994: The Operational Recognition of Supercell Thunderstorm Environments and Storm Structures. Wea. Forecasting, 9, 327-347.
- Piaget, A., L'évolution orageuse au nord des Alpes et la tornade du Jura Vaudois du 26 août 1971, Publ. 35, SZ ISSN 0080-7346, 102 pp., L'inst. Suisse de Météorol., Payerne, Switzerland, 1976.
- Schmid, W., H.-H. Schiesser, B. Bauer-Messmer, 1997: Supercell storms in Switzerland: Case studies and implications for nowcasting severe winds with Doppler radar. Meteor. Appl., 4, 49-67.
- Uccellini L. W., and D. Johnson, 1979: The coupling of upper and lower tropospheric jet streaks and implications for the development of severe convective storms. Mon. Wea. Rev., 107, 682–703.
- Taszarek, M., N. Pilguj, J. Orlikowski, A. Surowiecki, S. Walczakiewicz, W. Pilorz, K. Piasecki, Ł. Pajurek, M. Półrolniczak, 2019 : Derecho evolving from a mesovortex – A study of 11 August 2017 severe weather outbreak in Poland : event analysis and high-resolution simulation. Mon. Wea. Rev., 147, 2283-2306.
- Weisman, M.L., Klemp, J.B., 1982: The dependence of numerically simulated convective storms on wind shear and buoyancy. Mon. Wea. Rev., 110, 504-520.